CFD CORRECTED STATIC AEROELASTIC STIFFNESS OPTIMIZATION OF A PASSENGER AIRCRAFT WING

J. Dillinger, DLR - Institute of Aeroelasticity, Germany
P. Cabral, Embraer S.A., Brazil
G. Silva, Embraer S.A., Brazil
A. Prado, Embraer S.A., Brazil
Y. Meddaikar, DLR - Institute of Aeroelasticity, Germany

ABSTRACT

This paper presents the application of a static aeroelastic stiffness optimization process to a passenger-type aircraft wing. In order to improve the aeroelastic load calculation, which is typically based on a doublet lattice panel method, a computational fluid dynamics (CFD) correction method is applied. The wing geometry and the corresponding shell finite element model of the load carrying structure are generated with *ModGen*, a parametric model generator used in combination with the finite element code *Nastran*. Design variables in the gradient based optimization process are the membrane and bending stiffness matrices **A** and **D**. Shell elements are grouped in so-called design fields in wing skins and spars, each of which features a unique set of stiffness matrices. The responses to be considered in the optimization consist of the classical structural quantities mass, strain and buckling, as well as the aeroelastic constraints aileron effectiveness, divergence and twist.
The optimization is based on the minimization of an approximated sub-problem. To this end, linear and reciprocal approximations of the responses to be considered are set up, relying on the response sensitivities evaluated with *Nastran*. After a successful minimization of the local problem, the new set of design variables serves as an input for the generation of a new local approximation problem. The loop is repeated till convergence of the optimization objective.
Results are presented for various combinations of responses and laminate types. While mass is always the optimization objective, optimizations with and without aileron effectiveness, as well as for balanced and unbalanced laminates are discussed. In order to assess the influence of the CFD correction on the optimization results, each optimization set is performed with and without correction.

1. INTRODUCTION

In search of evermore efficient aircraft systems, one of the key components certainly is the introduction of new and more efficient materials, which in the past and up to today has strongly been addressed by composite materials.
With the application of composite materials in load carrying structures of modern passenger type aircraft, the optimization techniques need to be adopted, if not redeveloped according to the specific material characteristics. The books [1] and [2] yield detailed insight into composite optimization in particular and structural optimization in general.
The identification of potential benefits to be achieved with composites applied to aircraft wings in particular, has entailed a considerable amount of research work, see for example [3], where the authors apply an approximation based optimization to minimize the weight of a wing structure subjected to different combinations of buckling, strength, displacement and twist constraints.
In [4], Vanderplaats and Weisshaar provide a general overview on optimization technologies reaching from optimizations on panel level to the aeroelastic optimization of composites in aircraft wings.
In [5], Ringertz performs a mass optimization for a cantilevered beam subjected to aeroelastic loads derived from doublet lattice methods. The thicknesses of the unbalanced wing skin laminates serve as design variables, with the wing being subjected to divergence and flutter constraints. Subsequently, the design is analyzed for imperfection sensitivity.
The influence of layup orientation in a straight fiber design on the optimized mass of a low aspect ratio wing that is constrained by strength, roll-reversal and flutter velocity is shown by Eastep *et al.* [6]. More recent works [7], [8], [9] focus on dynamic aspects such as eigenmodes, flutter and gust responses in the analysis and optimization of

composite wings with various optimization techniques.

By means of so-called lamination parameters, another possibility exists to express laminate stiffness matrices based on a limited set of continuous variables rather than stacking sequence parameters like ply number, angle, and thickness.
They were first introduced by Tsai *et al.*, [10], [11], and represent an integral form of the discrete composite stack stiffnesses.
Aeroelastic tailoring studies based on lamination parameters have been attempted previously. In [12], Kameyama and Fukunaga by means of a symmetrically stacked composite plate wing demonstrate the influence of lamination parameters, describing the bending stiffness matrix, on the flutter and divergence characteristics. Moreover they demonstrate a genetic algorithm based weight optimization with constraints on divergence and flutter speeds.
Beam and shell based stiffness optimizations on the basis of lamination parameter are described in [13], [14], addressing also the influence of unbalanced variable stiffness laminates on weight optimized wing designs.
In [15], Thuwis *et al.* demonstrate the possibility of reducing the induced drag of a Formula One wing using passive twist adaption resulting from an aeroelastic tailoring optimization based on lamination parameters.
Another two-level optimization strategy has been proposed in [16]. Allowing for symmetric and unbalanced laminates, a lamination parameter based weight minimization is performed, followed by a genetic algorithm based derivation of the stacking sequences.
In [17], Dillinger *et al.* describe a stiffness optimization strategy based on lamination parameters and the consideration of static aeroelastic constraints. The strategy is adopted in the stiffness optimization of a parametrically defined set of forward swept wings, [18], featuring equivalent wing area and span and variable leading edge sweep. The influence of several static aeroelastic constraints on the minimized wing skin mass is investigated, in particular focusing on potential benefits of unbalanced over balanced laminates. Steady aeroelastic loads are calculated with a doublet lattice method (DLM) embedded in the applied finite element solver, allowing for the generation of response sensitivities that incorporate the effects of displacement-dependent, aeroelastic loads.
To incorporate flow phenomena that cannot be reproduced with DLM, the optimization process was extended by a correction method featuring a higher order aerodynamic method.
The correction is twofold, firstly aiming at a correction of DLM by means of camber and twist modifications applied directly to the doublet lattice mesh and secondly, by employing the capabilities of a higher order computational fluid dynamics (CFD) solver, like the DLR-based TAU code. To this end, DLM loads transferred to the structure are corrected by means of higher-fidelity CFD results. An application of the process is shown in [19], while a detailed description of the entire optimization framework including aero load correction is given in [20].

This paper describes the application of the optimization process including aero load correction to a passenger type aircraft wing. The work was performed in the course of a project initiated by EMBRAER S.A., called "Embraer Aeroelastic Tailoring Project", involving various international research and development institutions.
The aim is to demonstrate and enhance sundry aeroelastic tailoring and composite related topics, tools and research branches. To this end, a common benchmark aircraft model is provided by EMBRAER S.A., involving geometrical, structural, aerodynamic, mass, material and load case related data allowing for the generation of various analysis models. The aircraft model addresses mainly composite wing related data, including finite element representations with different optimization model fidelity levels.
The project is a direct successor to the "Embraer Composite DD-WING" project, which involved the fundamental demonstration of the static aeroelastic tailoring process developed at DLR, based on an initial version of the benchmark aircraft described above.

2. OPTIMIZATION PROCESS OVERVIEW

The static aeroelastic stiffness optimization process, as developed at the DLR – Institute of

Aeroelasticity (DLR-AE) is depicted in Figure 1. A detailed description of the optimization process can be found in [17].
The framework consists of a successive convex subproblem iteration procedure, in which a gradient based optimizer consecutively solves a local approximation problem. Responses are approximated as a linear and/or reciprocal function of the laminate membrane and bending stiffness matrices **A** and **D**. Together with the laminate thicknesses h, they constitute the design variables in the optimization process.

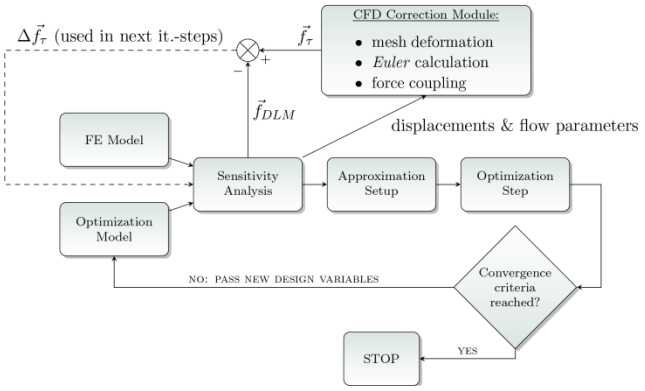

Figure 1: Static aeroelastic optimization process

The distribution of design fields - each of which comprises its own set of **A**, **D**, h variables – within a structural entity like a wing skin, determines the variable stiffness resolution. Inside the optimization algorithm, stiffness matrices are parameterized by means of lamination parameters, resulting in a reduction in the amount of design variables on the one hand, and the constitution of a continuous, well-posed optimization problem on the other.
The response sensitivities with respect to the design variables form an essential input in the assembly of response approximations. In this research, the finite element (FE) software *Nastran* is applied in order to generate sensitivities. Three major reasons account for this choice: one, the ability of specifying various types of responses, two, the time efficient implementation, and three, its prevalence in the aircraft industry.
Structural responses considered in the stiffness optimization are strength, buckling and mass; aileron effectiveness, divergence, and twist constitute the aeroelastic responses.

3. CFD CORRECTION METHODS

The reason to include an aero load correction in the structural optimization of an aircraft relates mainly to the fact that aeroelastic forces as generated by the commonly used doublet lattice method (DLM) cannot consider the occurrence of local recompression shocks. In summary, three main reasons can be addressed for a correction:

- compressibility effects including local recompression shocks,
- airfoil camber and thickness as opposed to the standard flat plate results obtained from DLM,
- strongly non-linear aerodynamic forces resulting from viscous flow phenomena like separation.

In order to lower the computational costs, for now a CFD Euler solution was considered rather than RANS or even higher order methods. Euler however cannot capture the viscous flow phenomena addressed in the above list. Nevertheless, the modularity of the implemented CFD correction process allows for an easy exchange of the CFD solution with higher order methods and might be addressed in future work.

Typically, aeroelastic loads for regular aircraft configurations are computed within *Nastran* by means of the built-in doublet lattice method. Eventually, it is possible to directly relate the local downwash angle w_j to the pressure p_j in each panel, and thus to the aerodynamic force either on panel level, f_a, or transferred to the structural model, f_{DLM}:

$$w_j = {}^1/_q \, AIC_{jj} p_j \tag{1}$$

$$f_a = S_{aj} p_j \tag{2}$$

$$f_{DLM} = H_{sa} f_a \tag{3}$$

where q, S and H are the dynamic pressure, panel area and spline function, respectively. The aero load correction process as applied in the present investigation is twofold, addressing different terms in equations (1) to (3). One part consists of a

camber correction applied to each individual aerodynamic panel. To this end, *Nastran* provides a correction matrix $w2gj$ that adds an additional term to the local downwash angle w_j in equation (1):

$$(w_j + w2gj) = {}^{1}/_{q}\, AIC_{jj} p_j \tag{4}$$

The required box rotations for the emulation of a camber line are shown in Figure 2(a). The chordwise constant rotation of each DLM box as shown in Figure 2(b) is used to emulate a twist of the wing section.

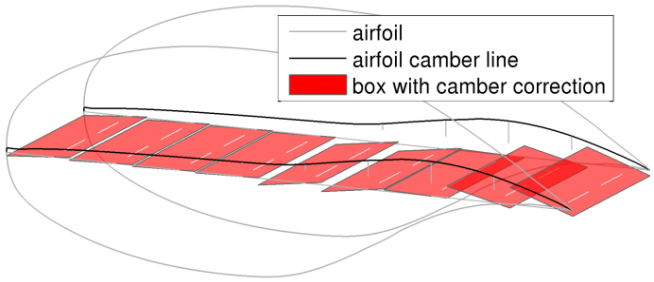

(a)

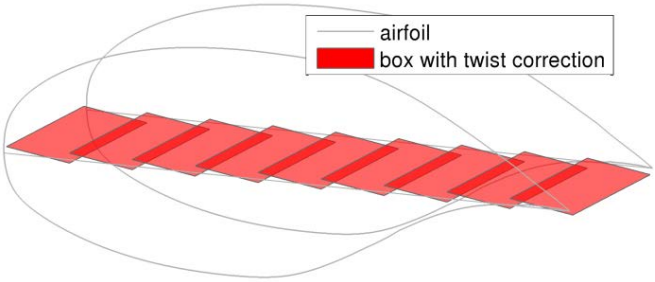

(b)

Figure 2: DLM $w2gj$ correction illustration

The second aero load correction part consists of rectifying aerodynamic loads obtained using the doublet lattice method, f_{DLM}, using CFD results, f_τ:

$$\Delta f_\tau = f_\tau - f_{DLM} \tag{5}$$

The difference Δf_τ between the CFD force vector and the DLM force vector at each coupling node is applied as a static correction in equation (3). A sample of force vectors on a deformed wing structure are shown in Figure 3.

It should be noted that the interdependency of aerodynamic loading and structural deformation necessitates an iterative procedure to compute the balanced aerodynamic loading on the wing structure. A detailed description of the entire aero load correction process is provided in [20].

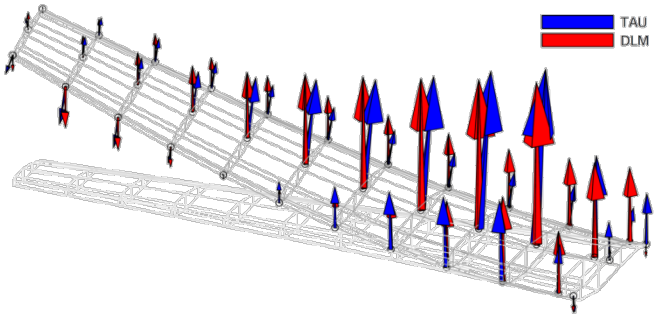

Figure 3: Force vectors at the coupling nodes

4. FINITE ELEMENT MODEL AND OPTIMIZATION MODEL

The optimization models are created with the parametric pre-processing tool *ModGen*, [21]. *ModGen* generates the *Nastran* input files representing the wing structure in three separate runs, one for each of the three components main wing box, landing gear box and center wing box. They are combined to a single entity by equalizing nodes at the entity boundaries.

Also the doublet lattice model, as well as the coupling model between structural and aerodynamic model are generated with *ModGen*. The full analysis model is depicted in Figure 4.

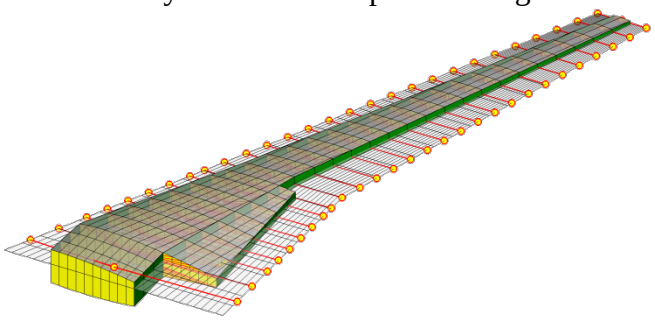

Figure 4: Full *Nastran* analysis model

The definition of the optimization model basically consists of a selection of design variables and responses, one of which will become the optimization objective. Design variables in the applied gradient based optimization process are the membrane and bending stiffness matrices **A** and **D**. Shell elements are grouped in so-called design fields in wing skins and spars, each of which features a unique set of stiffness matrices. The design field distribution considered in the present optimizations is depicted in Figure 5

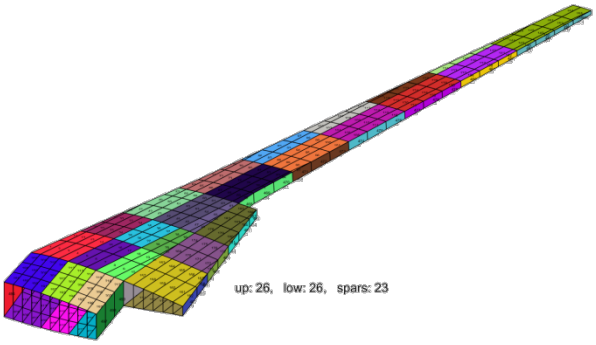

Figure 5: Design fields in the optimization model

Upper and lower wing skin feature 26 design fields each, plus an additional 23 fields in the spars. Along with the six design variables for the representation of a stiffness matrix and the thickness of a design field, in total $(2 * 26 + 23) * (2 * 6 + 1) = 975$ design variables are defined.
The responses to be considered in the optimization consist of the classical structural quantities mass, strain and buckling, as well as the aeroelastic constraints aileron effectiveness, divergence and twist.

4.1 LOAD CASES

The maneuver load cases (LC) considered in the optimization and hence also required to be included in the aero load correction process are listen in Table 1.

Table 1: Load case definition

load case	mass	EAS, m/s	Mach	Altitude, [m]	n_z, g
01	Fuel	145.9	0.820	10000	2.50
02	Fuel	131.9	0.879	11887	1.88
03	Empty	123.0	0.820	11887	-1.00
04	Empty	162.0	0.576	3048	-1.00
05	Fuel	142.2	0.500	3048	2.50

Eventually, a complete load case number consists of four digits, where the last two digits identify the load case as addressed in Table 1 and the first two digits the mass case. These combined LC numbers will be used in the result presentations later on.

5. OPTIMIZATION

In order to estimate the influence of aero load correction on the minimum achievable structural wing box mass, an optimization study was performed.
The calculations were performed for strain allowables in tension, compression, shear of $[0.45_{\varepsilon t}$ / $-0.45_{\varepsilon c}$ / $0.7_{\gamma xy}]$%, lowered by a safety factor of 1.5. Buckling would occur at 66% of the applied load rather than at the regular 100%. This work-around was introduced to simulate the effect of ultimate loads compared to maximum loads, which was not yet implemented in the optimization framework.
Starting with a mass minimization with only structural constraints strain and buckling, but without aeroelastic constraints, results were generated for balanced and unbalanced laminates. To substantiate the resulting minimized mass found in an optimization, each optimization was rerun with a second starting point.
The second set of optimizations then comprised the same set of constraints, but with the aero load correction turned on; again, balanced and unbalanced laminates, as well as two different starting points. The two sets described above were complemented by an additional aeroelastic constraint, aileron effectiveness, resulting in two additional optimization sets.
The minimized structural wing masses for all four sets - normalized with respect to the optimum obtained for set 1, balanced laminates, and for the starting point (SP) that lead to the minimum result - are summarized in Table 2.

Table 2: Minimized relative masses for various sets of constraints (strain and buckling responses active throughout)

	set	balanced	unbalanced
1	m_{min}	**100.0 %**	**92.8 %**
2	m_{min} + aero corr.	105.6 %	97.7 %
3	m_{min} + aileron eff. const.	100.6 %	96.3 %
4	m_{min} + aileron eff. const. + aero corr.	105.7 %	**98.9 %**

Table 2 indicates that aero load correction leads to an increase in optimized mass, however, this trend is quite model- and case-dependent.
Including aileron effectiveness as an additional constraint leads to a mass increase, noting that the difference is only marginal in case of balanced laminates. Eventually, unbalanced laminates in

general outperform balanced laminates by at least 4.3% and up to 7.2%.
The minimized masses highlighted in boldface in Table 2 will in the following be investigated in more detail.

5.1 PURE MASS MINIMIZATION WITHOUT AERO LOAD CORRECTION

Figure 6 shows the iterative mass development for a mass-minimization with unbalanced laminates, only structural constraints and without aero load correction. A mass increase from one iteration step to the next one indicates an infeasible design point, which the optimizer usually solves by a mix of thickness increase and stiffness direction adaptation.

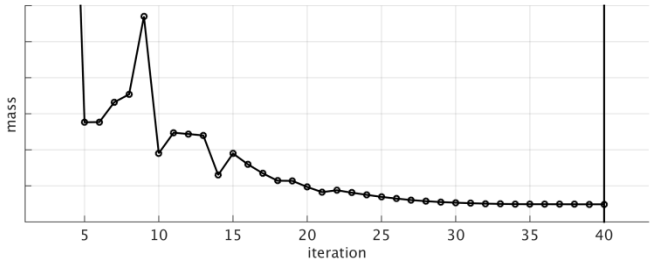

Figure 6: Iterative mass development, balanced laminates

Ultimately, the plot indicates a steady convergence towards a minimum, noting that the changes for the last ≈10 iteration steps are rather minimal.

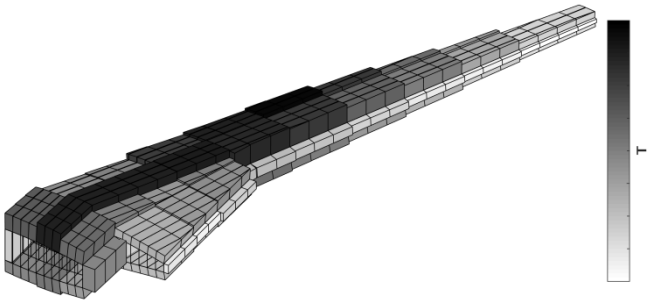

Figure 7: Optimized thickness distribution, unbalanced laminates

The corresponding thickness distribution is shown in Figure 7. The thickness decrease inside the kink is attributed to the bending moment relief due to the engine attached close to the kink, and the chord increase. The reduced chord in the center wing box again results in a thickness increase. The maximum thickness appears just outside the kink as a combined consequence of aeroelastic loads, wing box dimensions and secondary masses like the engine.
The optimized stiffness distribution in each design field is shown in Figure 8 for balanced and unbalanced laminates. The most prominent difference is the symmetrical versus unsymmetrical orientation of the stiffness distributions with respect to the 0° fiber angle direction (marked by black solid lines). The blue solid lines indicate the maximum stiffness direction, the light blue lines the minimum stiffness direction. In case of balanced laminates the maximum stiffness direction in the outer wing no longer points in spanwise (0°) but more in 45° direction, indicating that buckling, rather than strain constraints dominate the design fields sizing.

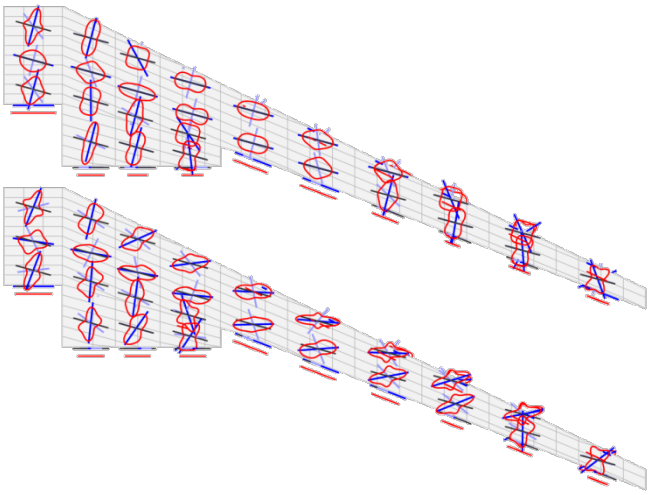
Figure 8: Stiffness distribution upper skin, balanced (upper) and unbalanced (lower) laminates

It can be observed that mainly the middle row (in chordwise direction) features a spanwise stiffness orientation while the design fields fore and aft do not. This can be accredited to the fact that the middle row is situated in the area of largest airfoil thickness and thus is the most effective in terms of bending stiffness control.
The same effect of spanwise directing stiffnesses in the middle row can be found for the unbalanced design; however, the distributions clearly indicate a gradual forward tilting of the main stiffness direction when moving outward in spanwise direction. The freedom of tilting the main stiffness direction is possible in unbalanced laminates and in the present case leads to the typical aeroelastic tailoring effect of bending torsion coupling. Eventually, bending the wing up couples with a nose-down twisting and thus provides a load relief in the outer wing. This in turn is beneficial in the search for a mass-minimized design, since it ultimately leads to reduced bending moments in the wing root area.
For the case with unbalanced laminates the optimization history for aileron efficiencies

resulting from four roll maneuver simulation conditions are shown in Figure 9. A negative aileron effectiveness response implies aileron reversal and thus an impermissible flight condition. The design ultimately shows aileron reversal for three load cases.

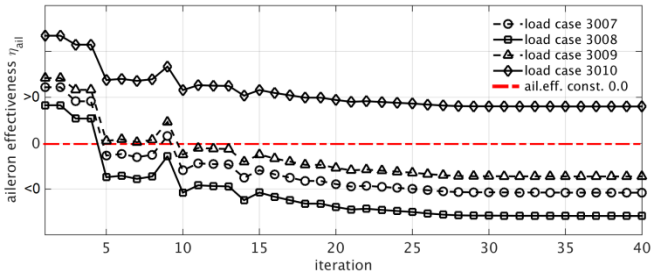

Figure 9: Aileron effectiveness development, unbalanced laminates

Representations of the failure indices in upper skin (elements 1-217), lower skin (elements 218-434), and spars (elements 435-499) are shown in Figure 10. For strain (red), a failure index of 1.0 is the boundary towards failure, while for buckling (blue) the boundary is at 0.667, with values above indicating failure.

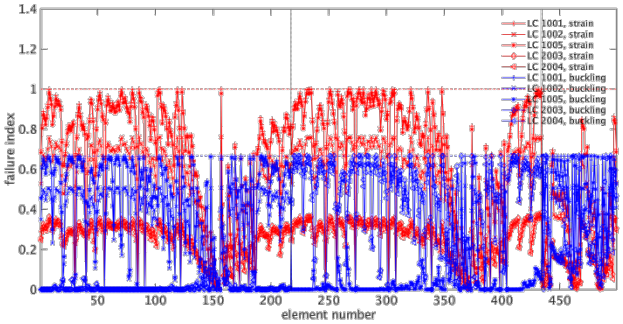

Figure 10: Failure indices, balanced laminates

It is noticeable that more elements are sized by buckling than by strain failure, especially in the inner and outer wing region, where strain failure indices drop below 1.0. Nevertheless in large portions of the wing a simultaneous failure in strain and buckling is predicted, suggesting a maximum material exploitation and thus weight optimal designs.

5.2 MASS MINIMIZATION WITH AERO LOAD CORRECTION AND AILERON EFFECTIVENESS CONSTRAINTS

In this section, results for an optimization including not only aileron effectiveness constraints, but also aero load correction are presented. Focus will be placed on the results with unbalanced laminates.

Compared to the previous optimization set without aileron effectiveness constraints and without aero load correction the optimized structural wing mass increased by ≈ 6 % (Table 2), mainly due to the imposed aileron effectiveness constraint (Figure 11).

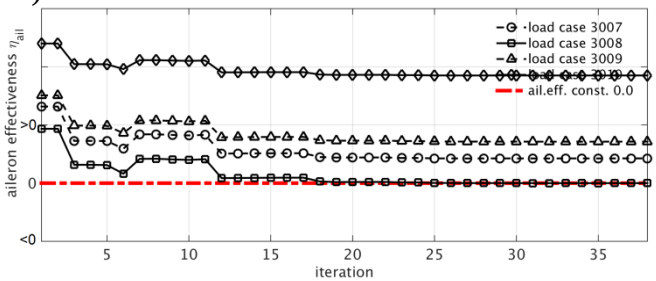

Figure 11: Aileron effectiveness development, unbalanced laminates

The optimizer is able to maintain an aileron effectiveness equal or larger than zero, thus no aileron reversal occurs for the investigated load cases.

Characteristics of the optimized thickness distribution, Figure 12, were maintained (compare Figure 7), and only minor changes in the stiffness distributions of the upper skins were required to achieve the imposed aileron effectiveness constraint, seen in Figure 13 as compared to Figure 8 (lower plot).

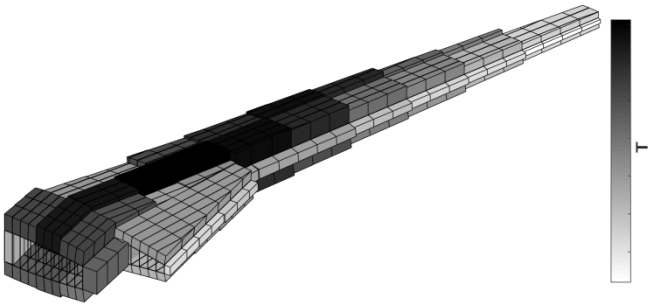

Figure 12: Optimized thickness distribution, unbalanced laminates

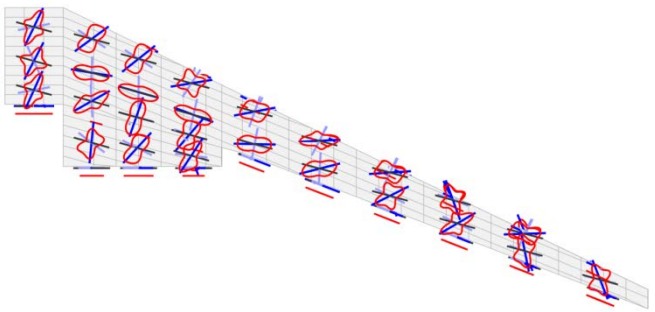

Figure 13: Stiffness distribution upper skin, unbalanced laminates

The effect of aero load correction consideration can be best addressed in a comparison of a low *Mach* number flight case and a high *Mach* number

flight case. The chordwise pressure difference between upper and lower airfoil side resulting from *Nastran* internal doublet lattice solution and the external TAU *Euler* solution for such two solutions are provided in Figure 14 and Figure 15.

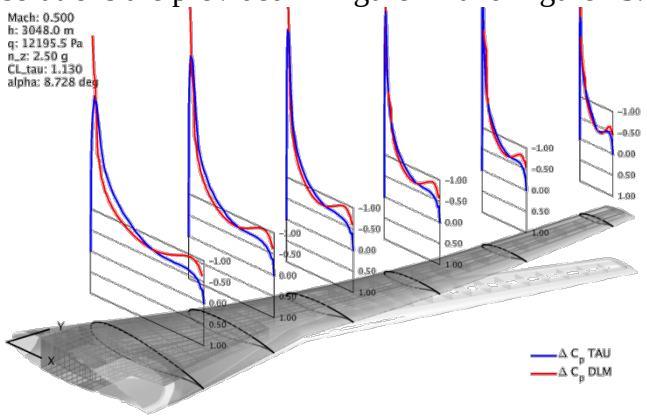

Figure 14: Pressure difference comparison, optimized solution, low Mach number LC 1005

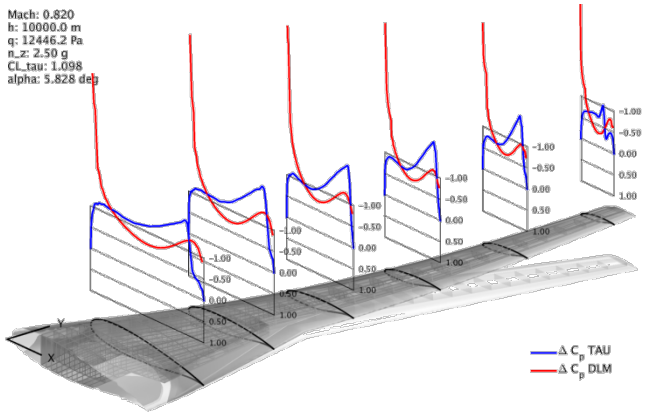

Figure 15: Pressure difference comparison, optimized solution, high Mach number LC 1001

The effect of camber correction is clearly visible in the doublet lattice results by means of the characteristic rear loading distribution. An uncorrected DLM solution would steadily develop towards $\Delta C_p = 1.0$ at the trailing edge. However, it can be seen that the characteristics of the doublet lattice solution do not change with increasing Mach number.

The TAU solution on the other hand completely changes its characteristics when going from lower to higher *Mach* numbers. The reason for this are recompression shocks (and areas with locally M>1). Obviously, the deviations in ΔC_p between DLM and TAU depicted in Figure 15 lead to deviations in the spanwise aerodynamic force and moment distribution. These differences are addressed in the lift and moment coefficient distributions in Figure 16. The wavy distribution in the kink-area is a result of variations in the integration area that had to be used to sum up the lift forces in order to compute the coefficients.

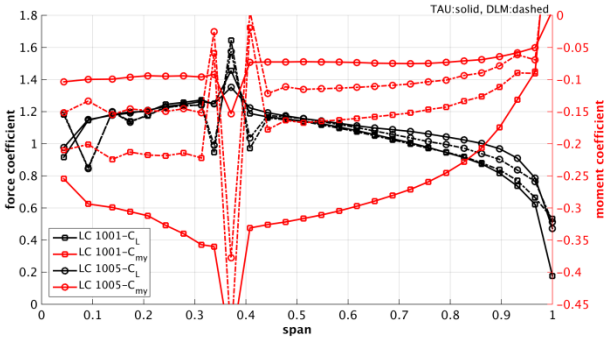

Figure 16: Lift- and moment coefficient comparison, optimized solution

It is interesting to note that the force coefficient for the higher Mach number LC 1001 shows closer resemblance of DLM and TAU as compared to the lower Mach number, LC 1005. This can be attributed to the fact that the overall force coefficient (which is proportional to the area below the curve) for LC 1001 and LC 1005, DLM and CFD all need to be the same, given that the lift to be generated is identical. The absolute difference in moment coefficient between DLM and TAU on the other hand considerably increases with the higher *Mach* number.

Eventually, in order to prove convergence of the TAU correction process, Figure 17 shows the force development in the course of structural iterations. From iteration step 27 onward the correction force remains nearly constant, as did the optimized wing mass (not shown). It should be noted that TAU correction forces are updated only every 4th iteration, indicated by the vertical solid lines. This proved to be an adequate trade-off between computational costs for the CFD calculation and convergence behavior.

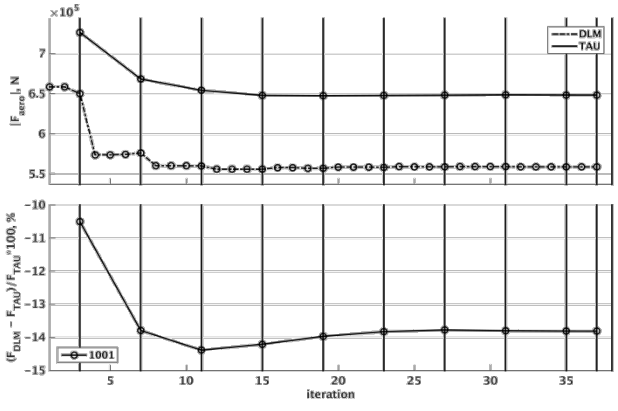

Figure 17: Aeroelastic loads convergence

6. CONCLUSIONS

A detailed analysis of the influence of aero load correction and an aileron effectiveness constraint on the optimization results has been presented. Even though the application of the correction does not necessarily have to show a definite trend, in the present investigation, for all optimization sets performed the consideration of aero load correction led to an increase of wing structural mass.

ACKNOWLEDGEMENTS

The research for this paper was initiated and greatly supported by the "Embraer Aeroelastic Tailoring Project", led by EMBRAER S.A and financially supported by the DLR – Institute of Aeroelasticity. In developing the ideas presented here, we have received helpful input from both parties.

REFERENCES

[1] Z. Gürdal, R. T. Haftka and P. Hajela, Design and optimization of laminated composite materials, Wiley, 1999.

[2] R. T. Haftka and Z. Gürdal, Elements of structural optimization, Kluwer Academic Publishers, 1992.

[3] J. H. Starnes Jr and R. T. Haftka, "Preliminary Design of Composite Wings for Buckling, Strength, and Displacement Constraints," *Journal of Aircraft,* vol. 16, pp. 564-570, 1979.

[4] G. N. Vanderplaats and T. A. Weisshaar, "Optimum design of composite structures," *International Journal for Numerical Methods in Engineering,* vol. 27, pp. 437-448, 1989.

[5] U. T. Ringertz, "On structural optimization with aeroelasticity constraints," *Structural and Multidisciplinary Optimization,* vol. 8, pp. 16-23, 1994.

[6] F. E. Eastep, V. A. Tischler, V. B. Venkayya and N. S. Khot, "Aeroelastic tailoring of composite structures," *Journal of Aircraft,* vol. 36, pp. 1041-1047, 1999.

[7] D. M. Leon, C. E. Souza, J. S. O. Fonseca and R. G. A. Silva, "Aeroelastic tailoring using fiber orientation and topology optimization," *Structural and Multidisciplinary Optimization,* vol. 46, pp. 663-677, 2012.

[8] O. Stodieck, J. E. Cooper, P. M. Weaver and P. Kealy, "Improved aeroelastic tailoring using tow-steered composites," *Composite Structures,* vol. 106, pp. 703-715, 12 2013.

[9] S. Guo, D. Li and Y. Liu, "Multi-objective optimization of a composite wing subject to strength and aeroelastic constraints," *Proceedings of the Institution of Mechanical Engineers, Part G Journal of Aerospace Engineering,* vol. 226, pp. 1095-1106, 9 2012.

[10] S. W. Tsai and N. J. Pagano, Invariant properties of composite materials, Defense Technical Information Center, 1968.

[11] S. W. Tsai and H. T. Hahn, Introduction to Composite Materials, Technomic Publishing Co, 1980.

[12] M. Kameyama and H. Fukunaga, "Optimum design of composite plate wings for aeroelastic characteristics using lamination parameters," *Computers and Structures,* vol. 85, pp. 213-224, 2007.

[13] J. E. Herencia, P. M. Weaver and M. I. Friswell, "Morphing Wing Design via Aeroelastic Tailoring," in *48th AIAA/ASME/ASCE/AHS/ASC Structures, Structural Dynamics, and Materials Conference*, Waikiki, 2007.

[14] M. M. Abdalla, R. De Breuker and Z. Gürdal, "Aeroelastic Tailoring of Variable-Stiffness Slender Wings for Minimum Compliance," in *International Forum on Aeroelasticity and Structural Dynamics (IFASD)*, Stockholm, 2007.

[15] G. Thuwis, R. De Breuker, M. M. Abdalla and Z. Gürdal, "Aeroelastic tailoring using lamination parameters," *Structural and Multidisciplinary Optimization,* vol. 41, pp. 637-646, 2010.

[16] D. Liu and V. V. Toropov, "A lamination parameter-based strategy for solving an integer-continuous problem arising in composite optimization," *Computers & Structures,* vol. 128, pp. 170-174, 11 2013.

[17] J. K. S. Dillinger, T. Klimmek, M. M. Abdalla and Z. Gürdal, “Stiffness Optimization of Composite Wings with Aeroelastic Constraints,” *Journal of Aircraft*, vol. 50, pp. 1159-1168, 6 2013.

[18] J. K. S. Dillinger, M. M. Abdalla, T. Klimmek and Z. Gürdal, “Static Aeroelastic Stiffness Optimization and Investigation of Forward Swept Composite Wings,” in *10th World Congress on Structural and Multidisciplinary Optimization*, Orlando, 2013.

[19] J. Dillinger, M. M. Abdalla, Y. M. Meddaikar and T. Klimmek, “Static Aeroelastic Stiffness Optimization of a Forward Swept Composite Wing with CFD Corrected Aero Loads,” in *International Forum on Aeroelasticity and Structural Dynamics*, *IFASD 2015*, 2015.

[20] J. K. S. Dillinger, Static Aeroelastic Optimization of Composite Wings with Variable Stiffness Laminates, Dissertation, Delft, The Netherlands, 2014.

[21] T. Klimmek, “Parameterization of topology and geometry for the multidisciplinary optimization of wing structures,” in *CEAS 2009 - European Air and Space Conference*, Manchester, UK, 2009.

[22] J. Dillinger, “Advancement of a Composite Wing Optimization Process - Status Report 12 2016,” Göttingen, 2016.

[23] J. K. S. Dillinger, T. Klimmek, M. M. Abdalla and Z. Gürdal, “Stiffness Optimization of Composite Wings with Aeroelastic Constraints,” *Journal of Aircraft*, vol. 50, no. 4, pp. 1159-1168, jun, 2013.

[24] G. Silva, “BenchmarkWing_20151201_sent.zip,” 2016.